Journal of Sound and Vibration (2002) **249**(3), 447–463
doi:10.1006/jsvi.2001.3876, available online at http://www.idealibrary.com on IDEAL®

VIBRATION AND STABILITY OF ANNULAR PLATES IN NON-LINEAR CREEP CONDITIONS

A. GAJEWSKI

Institute of Physics, Cracow University of Technology, ul.Podchorążych 1, 30-084 *Kraków, Poland.*
E-mail: dantek@fizyk.ifpk.pk.edu.pl

(*Received* 4 *January* 2001, *and in final form* 1 *May* 2001)

This paper presents a study on the influence of the physical non-linearity of material in creep conditions on vibration and stability of non-uniform annular plates subjected to a follower force radially distributed at the outer edge. The stability analysis requires first the calculation of a membrane stress distribution and then the application of the kinetic stability criterion, making use of small superposed vibrations. The differential equations of the membrane and vibration states have been integrated by means of the transfer matrix method which allowed the determination of the relationships between the real and imaginary parts of the complex frequency and compressive force (characteristic curves). The results have been presented in numerous figures.

1. INTRODUCTION

Stability of elastic systems under non-conservative loading has already been studied for over 60 years by a number of authors. One of the earliest among them was Beck [1] who calculated the critical load in the case of tangential action of the force, i.e., when the direction of the force is always tangential to the axis of the deformed column at its free end. The literature devoted to the problems of analysis and synthesis of columns compressed by follower forces with respect to its stability has been discussed by Gajewski and Życzkowski [2], Bogacz and Janiszewski [3], Langthjem and Sugiyama [4–6] and others.

Recently, Koiter [7] strongly criticized papers of that type and stated that "The abundant literature on such *non-conservative* follower forces in the second half of the present century is devoid of any mechanism by means of which experiments on follower forces can be performed." However, to the author's knowledge, Yagn and Parshin [8] performed the first experimental verification of the loss of stability of a column compressed by the follower force in 1967. The results of those experiments confirmed Beck's [1] theoretical predictions well. Beck's column was also realized experimentally by Sugiyama *et al.* [9]. Their experiments also verified the flutter instability. Experimental verification of dynamic stability of vertical cantilevered columns subjected to a follower force and self-weight of the rocket motor is presented by Sugiyama *et al.* [10]. Recently, Langthjem *et al.* [11] during the Fourth EUROMECH Solid Mechanics Conference, June 26–30, 2000, Metz, France, presented a video recording of their interesting experiments concerning columns subjected to rocket thrust and a pipeline conveying fluid. The results were also in good agreement with theory. To recapitulate, one can be sure that the follower force is realistic, as Sugiyama *et al.* [12] showed in a Letter to the Editor.

The present paper deals with the analysis of vibration and dynamic stability of an annular plate with radially varying thickness subjected to a tangential follower force radially

0022-460X/02/030447 + 17 $35.00/0

distributed at the outer edge. The plate is assumed to be in creep conditions. Similar analysis problems for a linearly elastic annular plate were considered by Irie *et al.* [13], whereas the optimization problem was presented by Gajewski and Cupiał [14]. Recently, the influence of non-linear creep of material on vibrations and stability of a uniform column compressed by the tangential force and on the optimal shape of the column were examined by Gajewski [15, 16]. The problems of optimal design with respect to creep stability have been formulated mostly by Życzkowski [17] and his collaborators. Among them, the problem of optimal design with respect to creep buckling for in-plane loaded circular plates (but compressed by conservative forces) has been solved by Wróblewski [18] for the first time.

In most cases of non-conservative stability problems, the kinetic criterion of stability has to be applied. For this purpose, the small vibrations of an annular plate compressed by a follower force superposed on the membrane state should be analyzed. If real parts of all complex frequencies of vibration are negative, then the system is stable. If at least one of them is positive the system is unstable. If, however, the corresponding imaginary part of the frequency is not zero, then the vibrations pass from a decreasing amplitude to an increasing one and the system loses its stability by flutter (see, e.g., reference [2]). By the application of the transfer matrix method, the eigenvalues and the flutter loads of non-uniform annular plate are calculated numerically.

2. CONSTITUTIVE EQUATIONS OF CREEP STABILITY

Following the state equation hypothesis of Davenport [19], adapted by Wróblewski [18], it is assumed that the stress and strain components of a basic membrane stress state are interrelated by the following creep law, accounting for strain hardening:

$$\Phi(\bar{\sigma}_e, \varepsilon_e^c, \dot{\varepsilon}_e^c) = 0, \qquad \varepsilon_e^c = \varepsilon_e - \bar{\sigma}_e/\bar{E}, \qquad \varepsilon_e^2 = \tfrac{2}{3}\, e_{ij}e_{ij}, \qquad \bar{\sigma}_e^2 = \tfrac{3}{2}\, \bar{s}_{ij}\bar{s}_{ij}, \tag{1}$$

where ε_e^c denotes inelastic strain intensity, ε_e the total strain intensity, $\bar{\sigma}_e$ the stress intensity, $\bar{s}_{ij}$, e_{ij} are the stress and strain deviators. The dot denotes differentiation with respect to time and the bar over a symbol denotes dimensional quantity.

Among various creep stability theories the Rabotnov–Shesterikov [20] strain-hardening creep theory seems to be the most suitable here. Generally, it can be assumed that during vibrations of a system (or as a result of buckling), the stress and strain components in the basic membrane state are subject to small variations and a creep law (1) can be linearized with respect to them. The behaviour of the variations determines the stability of the basic state (precritical) at a critical time $\bar{t}^*$.The components of the stress and strain tensors will receive small increments $\delta\bar{\sigma}_{ij}$, $\delta\varepsilon_{ij}$ due to vibrations. Assuming the similarity of stress and strain deviators and incompressibility of material ($\varepsilon_{ij} = e_{ij}$), one can derive the constitutive equations for the vibrational state in the incremental form [18] as

$$\delta\bar{s}_{ij} = \frac{\bar{s}_{ij}}{\bar{\sigma}_e^2}\left(\frac{\delta\bar{\sigma}_e}{\delta\varepsilon_e} - \frac{\bar{\sigma}_e}{\varepsilon_e}\right)\bar{s}_{kl}\delta\varepsilon_{kl} + \frac{2}{3}\frac{\bar{\sigma}_e}{\varepsilon_e}\,\delta\varepsilon_{ij} = \frac{\bar{s}_{ij}}{\bar{\sigma}_e^2}(\bar{E}_t - \bar{E}_s)\bar{s}_{kl}\delta\varepsilon_{kl} + \frac{2}{3}\,\bar{E}_s\delta\varepsilon_{ij}. \tag{2}$$

In order to describe kinetic instability, one superposes small variations of the stress and strain state on the statical precritical membrane state. These variations satisfy the equation

$$\left.\frac{\partial\Phi}{\partial\dot{\varepsilon}_e^c}\right|_0 \delta\dot{\varepsilon}_e^c + \left.\frac{\partial\Phi}{\partial\varepsilon_e^c}\right|_0 \delta\varepsilon_e^c + \left.\frac{\partial\Phi}{\partial\bar{\sigma}_e}\right|_0 \delta\bar{\sigma}_e = 0. \tag{3}$$

Assuming that the variations of stress and strain components are in the form of small linear vibrations of complex frequency $\bar{\Omega} = \bar{\delta} + \mathrm{i}\bar{\omega}$:

$$\delta\varepsilon_e = \delta\varepsilon_e^a \, e^{\bar{\Omega}\bar{t}}, \qquad \delta\bar{\sigma}_e = \delta\bar{\sigma}_e^a \, e^{\bar{\Omega}\bar{t}}, \tag{4}$$

the tangent creep modulus, according to the Rabotnov–Shesterikov [20] theory, is equal

$$\bar{E}_t = \frac{\delta\bar{\sigma}_e}{\delta\varepsilon_e} = \frac{\delta\bar{\sigma}_e^a}{\delta\varepsilon_e^a} = \left(\bar{\Omega} \left.\frac{\partial \Phi}{\partial \dot{\bar{\varepsilon}}_e^c}\right|_0 + \left.\frac{\partial \Phi}{\partial \varepsilon_e^c}\right|_0 \right) \Big/ \left(\frac{\bar{\Omega}}{\bar{E}} \left.\frac{\partial \Phi}{\partial \dot{\bar{\varepsilon}}_e^c}\right|_0 + \frac{1}{\bar{E}} \left.\frac{\partial \Phi}{\partial \varepsilon_e^c}\right|_0 - \left.\frac{\partial \Phi}{\partial \bar{\sigma}_e}\right|_0 \right). \tag{5}$$

Therefore, the tangent creep modulus is a complex value, whereas the secant creep modulus $\bar{E}_s = \bar{\sigma}_e/\varepsilon_e$, which can be evaluated from equation (1), is a real value.

By analogy with the paper by Wróblewski and Życzkowski [21] our considerations are confined to the strain-hardening creep physical law suggested by Rabotnov [22]

$$\Phi(\bar{\sigma}_e, \varepsilon_e^c, \dot{\bar{\varepsilon}}_e^c) = \dot{\bar{\varepsilon}}_e^c (\varepsilon_e^c)^\mu - \Gamma \bar{\sigma}_e^n = 0, \tag{6}$$

where Γ, μ, n are material constants dependent on temperature. In this paper, the values for Cu 200°C are: $n = 32{\cdot}8$, $\mu = 9{\cdot}52$, $E_0 = 1{\cdot}22 \times 10^5$ MPa, $\Gamma = 2{\cdot}18 \times 10^{-113+n}$ $\mathrm{Mpa}^{-n}\mathrm{h}^{-1}$ (cf., reference [23]).

In the basic precritical state under the assumptions of constant stress $\bar{\sigma} = \mathrm{const}(t)$ and initial condition $\varepsilon_e^c(0) = 0$, one obtains from equation (1) and (6)

$$\varepsilon_e = (\bar{\sigma}_e/\bar{E}) \{1 + (\bar{E}/\bar{\sigma}_e)[(1+\mu)\Gamma \bar{\sigma}_e^n \bar{t}^*]^{1/(1+\mu)}\} \tag{7}$$

and the "secant modulus"

$$E_s = \bar{E}_s/\bar{E}_0 = \bar{E}/\bar{E}_0 \{1 + \bar{E}[(1+\mu)\Gamma \bar{t}^*]^{1/(1+\mu)} \bar{\sigma}_e^{(n-1-\mu)/(1+\mu)}\}. \tag{8}$$

The "tangent modulus" for the non-linear creep law (6) can be written in the form

$$E_t = \frac{\bar{E}(1 + ((1+\mu)/\mu)\bar{t}^*\bar{\Omega})}{\bar{E}_0\{1 + ((1+\mu)/\mu)\bar{t}^*\bar{\Omega} + (n(1+\mu)/\mu)\bar{t}^*\Gamma\bar{E}\ [(1+\mu)\Gamma\bar{t}^*]^{-\mu/(1+\mu)} \bar{\sigma}_e^{(n-1-\mu)/(1+\mu)}\}}. \tag{9}$$

It is a function of critical time $\bar{t}^*$ and of the complex frequency of vibration $\bar{\mathbf{\Omega}}$. $\bar{E}_0$ is a certain constant of stress dimension.

3. EQUATIONS OF THE MEMBRANE STATE

Consider an isotropic, non-uniform annular plate clamped at the inner edge and loaded by a follower force at the outer edge presented in Figure 1. The plate thickness is assumed to be circularly symmetric.

Hence, the in-plane membrane forces in the basic membrane state are uniformly distributed and also circularly symmetric. Only two components of the internal forces, namely, normal forces $\bar{N}_r$, $\bar{N}_\theta$ are not zero. By using the law of similarity of stress and strain deviators and assuming incompressibility of material, one can derive the dimensionless non-linear boundary value problem of the precritical state as

$$u' = -(1/2x)u + (3/4xhE_s)n, \quad n' = (hE_s/x)u + (1/2x)n, \quad u(\beta) = 0, \quad n(1) = 1,$$

$$n_r = (n/x), \quad n_\theta = (hE_s/x)u + (1/2x)n, \; n_e = \sqrt{(n^2/x^2) + n_\theta^2 - (n/x)n_\theta},$$

$$E_s = e/(1 + T(Pn_e/h)^{(n-1-\mu)/(1+\mu)}). \tag{10}$$

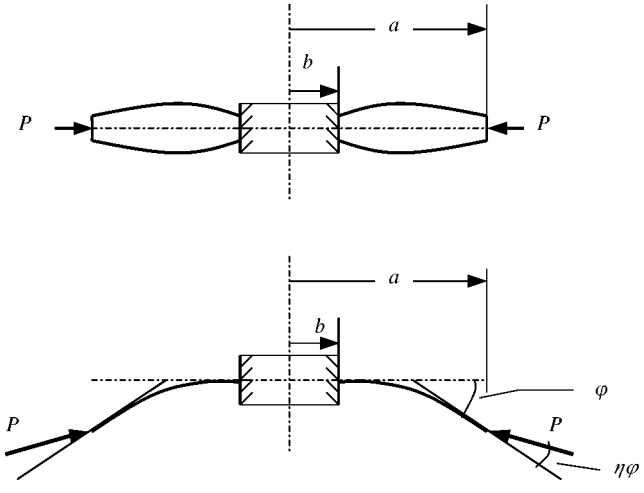

Figure 1. Non-uniform annular plate.

The dimensional quantities are related to the non-dimensional variables and parameters by the substitutions

$$\bar{r} = \bar{a}x,\ \bar{u} = -(\bar{P}\bar{a}/\bar{E}_0\bar{h}_0)u,\ \bar{N} = \bar{r}\bar{N}_r = -\bar{P}\bar{a}n,\ \bar{N}_r = -\bar{P}n_r,\ \bar{N}_\theta = -\bar{P}n_\theta,$$

$$\bar{P} = (\bar{E}_0\bar{h}_0^3/9\bar{a}^2)P, \qquad \beta = \bar{b}/\bar{a}, \qquad \alpha = \bar{h}_0^2/9\bar{a}^2, \qquad \bar{E} = \bar{E}_0 e(x), \qquad \bar{h} = \bar{h}_0 h(x). \tag{11}$$

4. EQUATIONS OF THE VIBRATION STATE

The well-known equation of small vibration superimposed on the membrane state of a plate may be written in the form

$$\frac{\partial^2(\bar{r}\bar{M}_r)}{\partial\bar{r}^2} + \frac{2}{\bar{r}}\frac{\partial^2(\bar{r}\bar{M}_{r\theta})}{\partial\bar{r}\partial\theta} + \frac{1}{\bar{r}}\frac{\partial^2\bar{M}_\theta}{\partial\theta^2} - \frac{\partial\bar{M}_\theta}{\partial\bar{r}} + \bar{r}\bar{N}_r\frac{\partial^2\bar{w}}{\partial\bar{r}^2}$$

$$+ \bar{N}_\theta\left(\frac{1}{\bar{r}}\frac{\partial^2\bar{w}}{\partial\theta^2} + \frac{\partial\bar{w}}{\partial\bar{r}}\right) - \bar{\gamma}\bar{r}\frac{\partial\bar{w}}{\partial\bar{t}} - \bar{\rho}\bar{r}\bar{h}\frac{\partial^2\bar{w}}{\partial\bar{t}^2} = 0, \tag{12}$$

where $\bar{w} = \bar{w}(\bar{r}, \theta, \bar{t})$ is the deflection of the plate and the increments of internal forces (superposed on zero initial values) are expressed as

$$\bar{M}_r = -\tfrac{1}{9}\bar{E}_s\bar{h}^3[a_{11}(\partial^2\bar{w}/\partial\bar{r}^2) + a_{12}((1/\bar{r})(\partial\bar{w}/\partial\bar{r}) + (1/\bar{r}^2)(\partial^2\bar{w}/\partial\theta^2))],$$

$$\bar{M}_\theta = -\tfrac{1}{9}\bar{E}_s\bar{h}^3[a_{21}(\partial^2\bar{w}/\partial\bar{r}^2) + a_{22}((1/\bar{r})(\partial\bar{w}/\partial\bar{r}) + (1/\bar{r}^2)(\partial^2\bar{w}/\partial\theta^2))],$$

$$\bar{M}_{r\theta} = -\tfrac{1}{9}\bar{E}_s\bar{h}^3 a_{33}(\partial/\bar{r})((1/\bar{r})(\partial\bar{w}/\partial\theta)). \tag{13}$$

The coefficients

$$\tilde{a} = \tfrac{3}{4}((\bar{E}_t/\bar{E}_s) - 1), \quad a_{11} = 1 + \tilde{a}(n_r^2/n_e^2), \quad a_{12} = a_{21} = \tfrac{1}{2} + \tilde{a}(n_r n_\theta/n_e^2),$$

$$a_{22} = 1 + \tilde{a}(n_\theta^2/n_e^2),\ a_{33} = \tfrac{1}{2} \tag{14}$$

are dependent on a critical time t^* and on the complex frequency of vibration. In the elastic case one has $\tilde{a} = 0$.

Now, one introduces the dimensionless variables and parameters.

Independent variables: $x = \bar{r}/\bar{a}, \qquad t = \bar{t}/\bar{t}_0,$

constant parameters: $\alpha = \bar{h}_0^2/9\bar{a}^2, \quad \bar{t}_0 = \sqrt{9\bar{\rho}_0\bar{a}^4/\bar{h}_0^2\bar{E}_0} = \sqrt{\bar{\rho}_0\bar{a}^2/\alpha\bar{E}_0},$

external force and frequency of vibration: $P = 9\bar{P}\bar{a}^2/\bar{E}_0\bar{h}_0^3, \ \bar{\Omega} = \bar{\Omega}\bar{t}_0,$

plate deflection and internal forces: $\tilde{w} = \bar{w}/\bar{a}, \ M_j = 9\bar{a}\bar{M}_j/\bar{E}_0\bar{h}_0^3, \ j = r, \theta, r\theta,$

mass density, external damping and Young's modulus distributions are, respectively:

$$\rho(x) = \bar{\rho}/\bar{\rho}_0, \quad \gamma(x) = \bar{\gamma}/\gamma_0, \quad e = \bar{E}/\bar{E}_0,$$

quantities connected with the physical law: $T_{00} = e[(1+\mu)\Gamma\bar{E}_0^n\bar{\tau}_0]^{1/(1+\mu)}\alpha_0^{(n-1-\mu)/(1+\mu)}$,

$$T = T_{00}(\bar{\tau}/\bar{\tau}_0)^{1/(1+\mu)}(\alpha/\alpha_0)^{(n-1-\mu)/(1+\mu)}, \quad E_s = \bar{E}_s/\bar{E}_0 = \frac{e}{1 + T(Pn_e/h)^{(n-1-\mu)/(1+\mu)}},$$

$$E_t = \bar{E}_t/\bar{E}_0 = e\frac{1 + ((1+\mu)/\mu)t^*\Omega}{(1 + ((1+\mu)/\mu)\,t^*\Omega + (n/\mu)T(Pn_e/h)^{(n-1-\mu)/(1+\mu)}},$$

$$\bar{\tau} = \bar{t}_0 t^* = \bar{t}^*, \ \bar{\tau}_0 = 3600 \text{ s}, \ \alpha_0 = 10^{-4}.$$

By considering the physical constants for copper and $e \equiv 1$, $T_{00} = 0{\cdot}781408$.

Next, the functions of the independent variables are separated and by using the substitutions suggested by Grinev and Filippov [24]

$$\begin{aligned} &\tilde{w}(x,\theta,t) = w(x)e^{\Omega t}\cos m\theta, \ \ M_r(x,\theta,t) = \tilde{M}_r(x)e^{\Omega t}\cos m\theta, \\ &M_\theta(x,\theta,t) = \tilde{M}_\theta(x)e^{\Omega t}\cos m\theta, \ \ M_{r\theta}(x,\theta,t) = \tilde{M}_{r\theta}(x)e^{\Omega t}\sin m\theta, \end{aligned} \tag{15}$$

$$\tilde{\tilde{M}}_r(x) = \tilde{M}_r(x) + \tfrac{1}{2}N_r(x)w(x), \tilde{\tilde{M}}_\theta(x) = \tilde{M}_\theta(x) + \tfrac{1}{2}N_\theta(x)w(x), \tilde{M}_{r\theta}(x) = \tilde{\tilde{M}}_{r\theta}(x), \tag{16}$$

$$\varphi = \mathrm{d}w/\mathrm{d}x = w', \ M = x\tilde{\tilde{M}}_r, \ Q = M' + 2m\tilde{\tilde{M}}_{r\theta} - \tilde{\tilde{M}}_\theta, \ N = xN_r = -Pn. \tag{17}$$

Therefore, equation (12) can be transformed to the set of four ordinary differential equations in non-dimensional form with complex coefficients:

$$w' = \varphi, \ \varphi' = \left(\frac{a_{12}}{a_{11}}\frac{m^2}{x^2} - \frac{Pn}{2a_{11}E_sh^3x}\right)w - \frac{a_{12}}{a_{11}}\frac{1}{x}\varphi - \frac{1}{a_{11}E_sh^3x}M,$$

$$M' = \left\{\left(2a_{33} + \frac{a_{11}a_{22} - a_{12}^2}{a_{11}}\right)E_sh^3\frac{m^2}{x^2} - P\left[\frac{1}{2}\left(\frac{1}{2} - \frac{a_{12}}{a_{11}}\right)\frac{n}{x} + \frac{1}{2}E_sh\frac{u}{x}\right]\right\}w$$

$$-\left(2m^2a_{33} + \frac{a_{11}a_{22} - a_{12}^2}{a_{11}}\right)\frac{E_sh^3}{x}\varphi + \frac{a_{12}}{a_{11}}\frac{1}{x}M + Q, \tag{18}$$

$$Q' = \left\{ m^2 \left(2a_{33} + m^2 \frac{a_{11}a_{22} - a_{12}^2}{a_{11}} \right) \frac{E_s h^3}{x^3} - P \left[m^2 \frac{E_s h}{x^2} u + \frac{m^2}{2x^2} \left(1 - \frac{2a_{12}}{a_{11}} \right) n + \frac{Pn^2}{4a_{11}E_s h^3} \right] \right\} w$$

$$+ (\gamma_0 \gamma x \mathbf{\Omega} + \rho x h \mathbf{\Omega}^2) w - \left\{ \left(2a_{33} + \frac{a_{11}a_{22} - a_{12}^2}{a_{11}} \right) E_s h^3 \frac{m^2}{x^2} \right.$$

$$\left. - P \left[\frac{1}{2} \left(\frac{1}{2} - \frac{a_{12}}{a_{11}} \right) \frac{n}{x} + \frac{1}{2} E_s h \frac{u}{x} \right] \right\} \varphi + \left(\frac{a_{12}}{a_{11}} \frac{m^2}{x^2} - \frac{Pn}{2a_{11}E_s h^3 x} \right) M.$$

To equations (18) one should add the boundary conditions. In the discussed case, the plate is rigidly clamped at the inner edge and non-conservatively loaded by the uniformly distributed force $\bar{P}$. Therefore, the boundary conditions can be written as:

$$w(\beta) = 0,\ \varphi(\beta) = 0,\ M(1) + \tfrac{1}{2} P w(1) = 0,\ Q(1) + (\eta - \tfrac{1}{2}) P \varphi(1) = 0, \tag{19}$$

where η denotes the tangency coefficient.

The boundary value problems (10) and (18), (19) determine the so-called characteristic curves, i.e., the relations between load parameter, P, and the real, δ, and imaginary, ω, parts of the complex frequency of vibration, $\mathbf{\Omega}$. In the case of non-conservative loading, the vibrations of the plate are stable if $\delta < 0$ and they lose stability by flutter if a real part of frequency changes its sign.

5. TRANSFER MATRIX METHOD

5.1. COMPLEX EQUATIONS

In order to obtain a solution of the boundary value problem (18), (19) one uses the transfer matrix method (see e.g., reference [13]). At first, equations (18) and (19) are rewritten in matrix form as

$$\mathbf{X}' = \mathbf{B}\mathbf{X},$$

where

$$\mathbf{X} = \{X_1,\ X_2,\ X_3,\ X_4\}^{\mathrm{T}} = \{w,\ \varphi,\ M,\ Q\}^{\mathrm{T}} \tag{20}$$

$$X_1(\beta) = 0,\ X_2(\beta) = 0,\ X_3(1) + \tfrac{1}{2} P X_1(1) = 0,\ X_4(1) + (\eta - \tfrac{1}{2}) P X_2(1) = 0,$$

and $\mathbf{B}$ is a matrix of coefficients in equation (18). The values of the state variables at arbitrary points x can be expressed by initial values at point $x = \beta$ by means of a matrix $\mathbf{S}(x)$ (the so-called transfer matrix)

$$\mathbf{X}(x) = \mathbf{S}(x)\mathbf{X}(\beta),\ \mathbf{S}(\beta) = \mathbf{1}. \tag{21}$$

Substituting equation (21) into equation (20) one obtains an initial problem which can be easily solved by numerical integration:

$$\mathbf{S}' = \mathbf{B}\mathbf{S},\ \mathbf{S}(\beta) = \mathbf{1}, \tag{22}$$

while boundary conditions (20) lead to the homogeneous algebraic linear equations for unknown boundary values $X_3(\beta)$, $X_4(\beta)$

$$[S_{33}(1) + \tfrac{1}{2}PS_{13}(1)]X_3(\beta) + [S_{34}(1) + \tfrac{1}{2}PS_{14}(1)]X_4(\beta) = 0,$$

$$[S_{43}(1) + (\eta - \tfrac{1}{2})PS_{23}(1)]X_3(\beta) + [S_{44}(1) + (\eta - \tfrac{1}{2})PS_{24}(1)]X_4(\beta) = 0. \tag{23}$$

For the existence of a non-trivial solution of equation (23), the determinant of the coefficient matrix must be zero. Therefore, the complex equation

$$[S_{33}(1)S_{44}(1) - S_{34}(1)S_{43}(1)] + \tfrac{1}{2}P[S_{13}(1)S_{44}(1) - S_{14}(1)S_{43}(1)] + (\eta - \tfrac{1}{2})P[S_{33}(1)S_{24}(1)$$
$$- S_{34}(1)S_{23}(1)] + \tfrac{1}{2}(\eta - \tfrac{1}{2})P^2[S_{13}(1)S_{24}(1) - S_{14}(1)S_{23}(1)] = 0 \tag{24}$$

determines the complex eigenvalue Ω as a function of tangency coefficient and other parameters of the problem. Moreover, from equation (23) one can calculate one of the boundary values, $X_3(\beta)$ or $X_4(\beta)$ under the assumption that the other one is known. But the differential equations (20) are homogeneous and either value may be arbitrarily chosen. For example,

$$X_4(\beta) = -([S_{33}(1) + \tfrac{1}{2}PS_{13}(1)]/[S_{34}(1) + \tfrac{1}{2}PS_{14}(1)])X_3(\beta),\ X_3^R = 1, X_3^I = 1. \tag{25}$$

5.2. REAL EQUATIONS

In order to simplify the calculations further one introduces new independent real variables and real matrices

$$\mathbf{Y} = \begin{Bmatrix} \mathbf{X}^R \\ \mathbf{X}^I \end{Bmatrix}, \quad \mathbf{A} = \begin{Bmatrix} \mathbf{B}^R & -\mathbf{B}^I \\ \mathbf{B}^I & \mathbf{B}^R \end{Bmatrix}, \quad \mathbf{T} = \begin{Bmatrix} \mathbf{S}^R & -\mathbf{S}^I \\ \mathbf{S}^I & \mathbf{S}^R \end{Bmatrix}. \tag{26}$$

Using equation (26) one obtains new boundary value problems with respect to new state variables $\mathbf{Y}$ and new transfer matrix $\mathbf{T}$

$$\mathbf{Y}' = \mathbf{AY},\ Y_1(\beta) = 0,\ Y_2(\beta) = 0,\ Y_5(\beta) = 0,\ Y_6(\beta) = 0,$$

$$Y_3(1) + \tfrac{1}{2}PY_1(1) = 0,\ Y_7(1) + \tfrac{1}{2}PY_5(1) = 0,$$

$$Y_4(1) + (\eta - \tfrac{1}{2})PY_2(1) = 0,\ Y_8(1) + (\eta - \tfrac{1}{2})PY_6(1) = 0. \tag{27}$$

$$\mathbf{T}' = \mathbf{AT},\ \mathbf{T}(0) = \mathbf{1} \text{ or } T'_{ij} = A_{i\alpha}T_{\alpha j},\ T_{ij}(0) = \delta_{ij},\ i, j, \alpha = 1, \ldots, 8, \tag{28}$$

where

$$\mathbf{Y}(x) = \mathbf{T}(x)\mathbf{Y}(\beta),\ \mathbf{Y}(1) = \mathbf{T}(1)\mathbf{Y}(\beta). \tag{29}$$

Complex equations (24) and (25) can be written as a set of real equations expressed by elements of real transfer matrix $\mathbf{T}$ as

$$[T_{33}(1)T_{44}(1) - T_{73}(1)T_{84}(1)] - [T_{34}(1)T_{43}(1) - T_{74}(1)T_{83}(1)]$$
$$+ \tfrac{1}{2}P\{[T_{13}(1)T_{44}(1) - T_{53}(1)T_{84}(1)] - [T_{14}(1)T_{43}(1) - T_{54}(1)T_{83}(1)]\}$$
$$+ (\eta - \tfrac{1}{2})P\{[T_{33}(1)T_{24}(1) - T_{73}(1)T_{64}(1)] - [T_{34}(1)T_{23}(1) - T_{74}(1)T_{63}(1)]\}$$
$$+ \tfrac{1}{2}(\eta - \tfrac{1}{2})P^2\{[T_{13}(1)T_{24}(1) - T_{53}(1)T_{64}(1)] - [T_{14}(1)T_{23}(1) - T_{54}(1)T_{63}(1)]\} = 0,$$

$$[T_{33}(1)T_{84}(1) + T_{73}(1)T_{44}(1)] - [T_{34}(1)T_{83}(1) + T_{74}(1)T_{43}(1)]$$
$$+ \tfrac{1}{2}P\{[T_{13}(1)T_{84}(1) + T_{44}(1)T_{53}(1)] - [T_{14}(1)T_{83}(1) + T_{43}(1)T_{54}(1)]\}$$
$$+ (\eta - \tfrac{1}{2})P\{[T_{33}(1)T_{64}(1) + T_{24}(1)T_{73}(1)] - [T_{34}(1)T_{63}(1) + T_{23}(1)T_{74}(1)]\}$$
$$+ \tfrac{1}{2}(\eta - \tfrac{1}{2})P^2\{[T_{13}(1)T_{64}(1) + T_{53}(1)T_{24}(1)] - [T_{14}(1)T_{63}(1) + T_{23}(1)T_{54}(1)]\} = 0 \tag{30}$$

and

$$Y_4(\beta) = -(aa/cc)\,Y_3(\beta) + (bb/cc)\,Y_7(\beta),\ Y_8(\beta) = -(bb/cc)\,Y_3(\beta) - (aa/cc)\,Y_7(\beta) \tag{31}$$

where

$aa = U_1V_1 + U_2V_2$, $bb = U_2V_1 - U_1V_2$, $cc = V_1^2 + V_2^2$, $U_1 = T_{33}(1) + \frac{1}{2}PT_{13}(1)$, $U_2 = T_{73}(1) + \frac{1}{2}PT_{53}(1)$, $V_1 = T_{34}(1) + \frac{1}{2}PT_{14}(1)$, $V_2 = T_{74}(1) + \frac{1}{2}PT_{54}(1)$.

Therefore, the determination of the transfer matrix elements $\mathbf{T}(x)$ allows for calculation of state variables $\mathbf{Y}(x)$ (real) as well as state variables $\mathbf{X}(x)$ (complex), the real and imaginary parts of frequency of vibration $\mathbf{\Omega}$. They generally depend on the compressive force P, tangency coefficient η, critical time $\bar{\tau}$, the number of circumferential waves m and other parameters of the problem. In particular, one can determine the critical value of the compressive force P which appears for $\delta = 0$.

6. NUMERICAL CALCULATIONS, RESULTS AND DISCUSSION

The numerical analysis was performed for a cantilever plate loaded by a tangential force ($\eta = 1$) uniformly distributed along the outer edge as shown in Figure 1(b). In all calculations, β was set to 0·2. The reference density $\bar{\rho}_0$ has been assumed to be equal to the plate density $\bar{\rho}$ and as a result $\rho \equiv 1$. Similarly $e \equiv 1$. The external damping has been neglected i.e., $\gamma_0 = 0$.

The dimensionless plate thickness is normalized according to the constant volume condition

$$\int_\beta^1 xh(x)\,\mathrm{d}x = \frac{\bar{V}}{2\pi\bar{a}^2\bar{h}_0} = 1, \tag{32}$$

where $\bar{V}$ is the volume of the plate, while the constant $\bar{h}_0$ equals $\bar{h}_0 = 3\bar{a}\sqrt{\alpha}$ for the chosen value of slenderness parameter α. In all calculations, $\alpha = 10^{-6}$. For a uniform plate the thickness is constant $h = 2{\cdot}083333$.

All differential equations were solved by the Runge–Kutta–Gill fourth-order integration method and the interval $[\beta, 1]$ was subdivided into 50 nodal points; the accuracy was checked by repeating the calculations with double the number of nodal points.

6.1. UNIFORM PLATE

Figures 2–4 present the typical behaviour of the characteristic curves corresponding to four frequencies of vibration for very small values of the critical time $\bar{\tau} = 10^{-6}$ s and for $m = 0$. The influence of the rheological properties of material is very small here and the

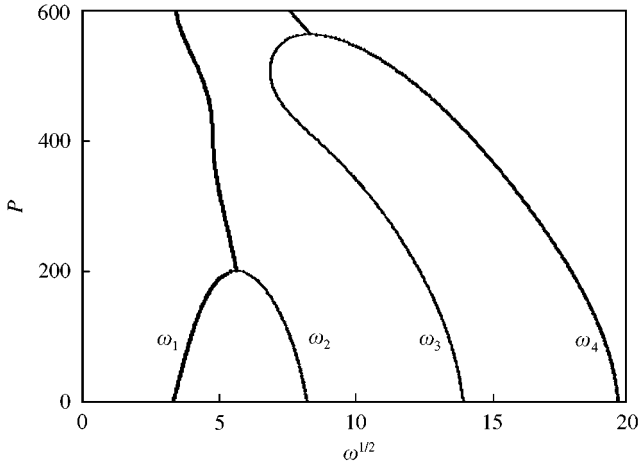

Figure 2. Compressive force P versus the imaginary part of the frequency of vibration ω for $\alpha = 10^{-6}$, $\bar{\tau} = 10^{-6}$ s and $m = 0$.

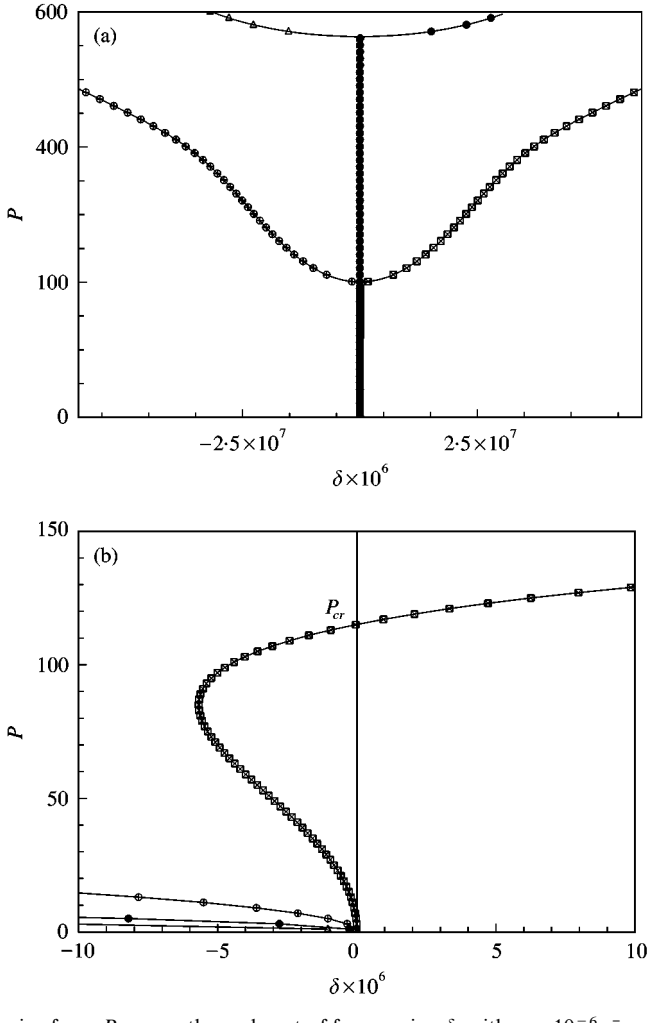

Figure 3. Compressive force P versus the real part of frequencies, δ, with $\alpha = 10^{-6}$, $\bar{\tau} = 10^{-6}$ s and $m = 0$, δ; ■—■, δ_1; ⊕—⊕, δ_2; ●—●, δ_3 and △—△, δ_4.

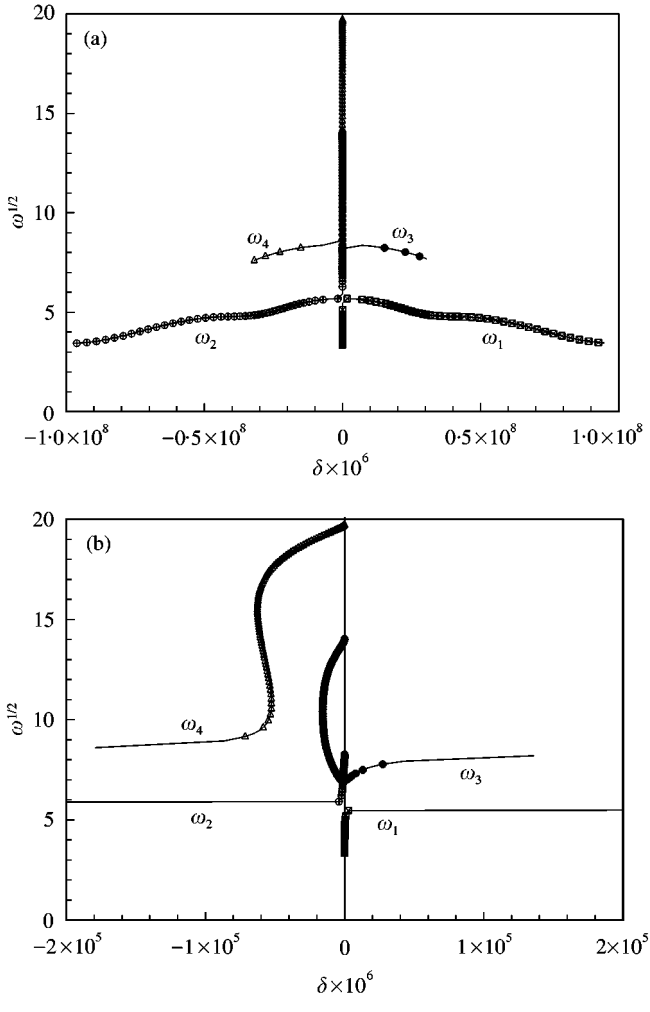

Figure 4. The imaginary part versus the real part of frequencies, ω, for $\alpha = 10^{-6}$, $\bar{\tau} = 10^{-6}$ s and $m = 0$, ω: ■—■,, ω_1; ⊕—⊕, ω_2; ●—●, ω_3 and △—△, ω_4.

curves $\omega - P$ are similar to those obtained by Gajewski and Cupiał [14] for elastic material. However, even for very small $\bar{\tau}$, the curves $\delta - P$ and $\delta - \omega$ should be analyzed. As it is seen in Figure 3(a), the first critical value of the compressive force P seems to be $P_{cr} \approx 200$ and the second one is $P_{cr} \approx 570$. But one can see in Figure 3(b) (which is an enlargement of a part of Figure 3(a)) that the real value of the frequency changes its sign for the first time at $P_{cr} \approx 114$. Therefore, the destabilization effect appears, which is similar to that observed for columns (see: e.g., references [6, 16]).

For larger values of critical time, the behaviour of the characteristic curves essentially changes. In Figures 5–7, the curves obtained for $\bar{\tau} = 0.1$ s and $m = 0$ are presented. The curves corresponding to the first and the second frequency of vibration separate. The critical value of the compressive force equals$P_{cr} \approx 125$ and it is reached only for the first frequency of vibration. The vibrations connected with other frequecies are stable in the range up to $P = 600$.

Of course, the characteristic curves depend also on the number of circumferential waves m. In Figure 8 the curves $\delta - P$ corresponding to the first frequency of vibration calculated

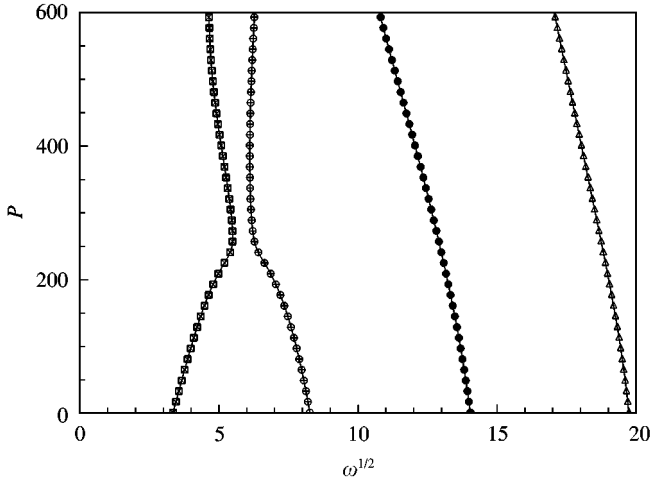

Figure 5. Compressive force versus the imaginary part of frequencies, ω, for $\alpha = 10^{-6}$, $\bar{\tau} = 0{\cdot}1$ s and $m = 0$, key as for Figure 4.

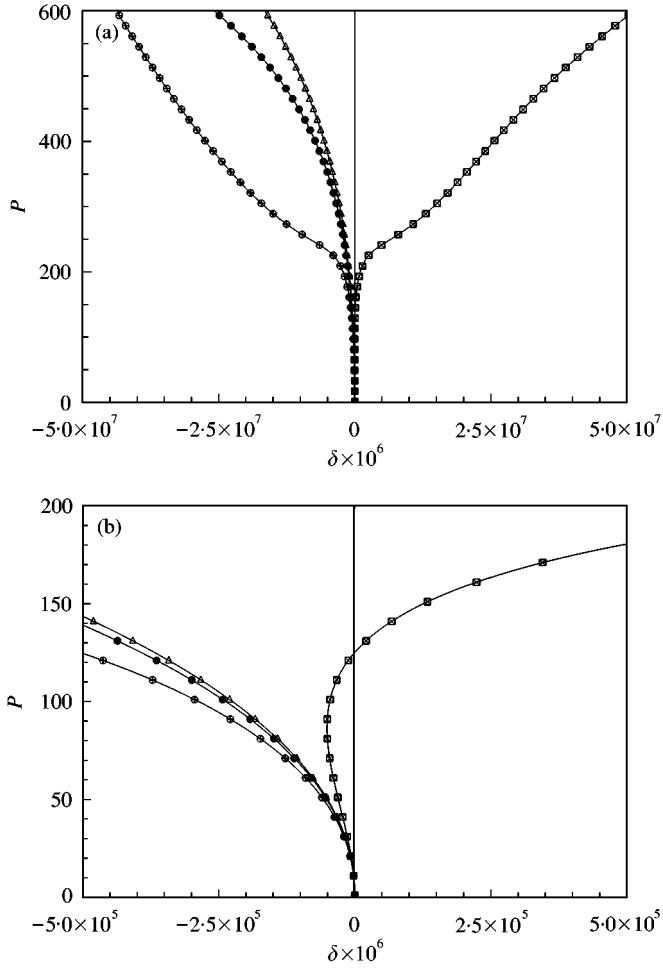

Figure 6. Compressive force versus the real part of frequencies, δ, for $\alpha = 10^{-6}$, $\bar{\tau} = 0{\cdot}1$ s and $m = 0$, key as for Figure 3.

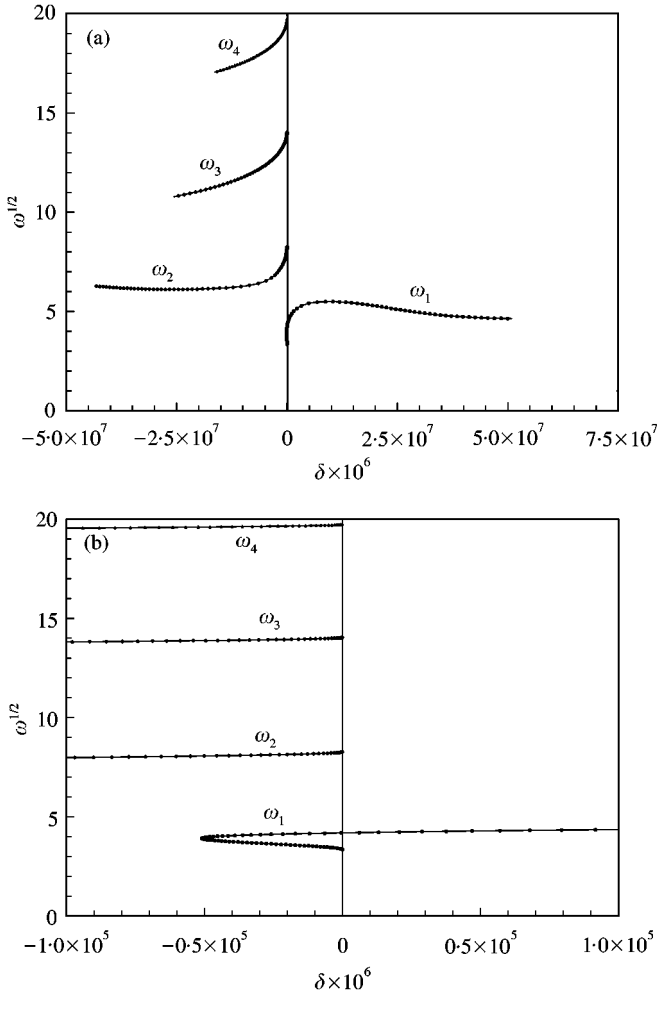

Figure 7. The imaginary part versus the real part of frequencies.

for $\bar{\tau} = 0{\cdot}001, 0{\cdot}1$ s and for $m = 0$–4 are presented. Finally, the curves $\omega - P$, corresponding to the first and the second frequency of vibration, for $\bar{\tau} = 0{\cdot}1$, 10 s for $m = 0$–4 have been plotted in Figure 9.

6.2. NON-UNIFORM PLATE—PARAMETRICAL OPTIMIZATION

In this section, the transfer matrix method is applied to annular plates with the thickness variation according to the power function

$$h(x) = h_1[1 - h_2((x - \beta)/(1 - \beta))s], \tag{33}$$

where h_1 is calculated from formula (34), so as to satisfy the normalization condition (32):

$$h_1 = \{\tfrac{1}{2}(1 - \beta^2) - h_2[(1 - \beta)^2/(s + 2) + \beta(1 - \beta)/(s + 1)]\}^{-1},\ s \neq 1,\ s \neq -2,\ h_2 \leqslant 1, \tag{34}$$

leaving two parameters free, namely, s and h_2.

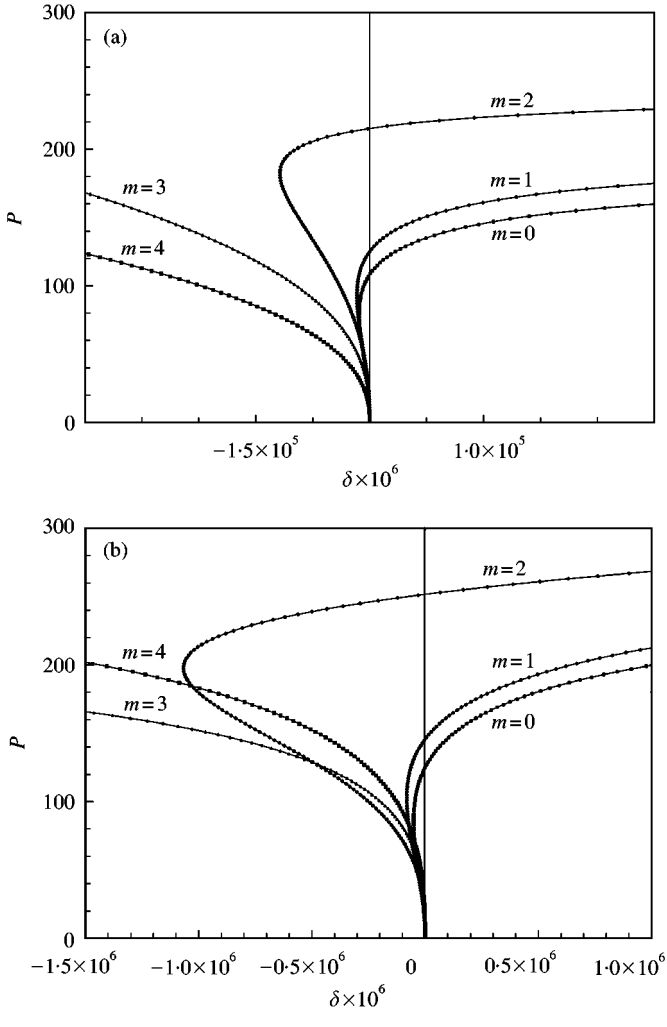

Figure 8. Compressive force versus the real part of frequencies with various values of m for (a) $\bar{\tau} = 0{\cdot}001$ s and (b) $\bar{\tau} = 0{\cdot}1$ s.

The eigenvalues of vibration and the critical flutter loads have been calculated numerically for $s = 1$ (linearly changing thickness), 2 (parabolically changing thickness) and also for $s = 3$ and 4·5. In Figure 10 the corresponding shapes of non-uniform plates are depicted. In all cases, the parameter h_2 changed from 0·2–0·9 (for $h_2 = 0$ represents a uniform plate), which allows one to determine the optimal value of h_2. The calculations were performed for $\bar{\tau} = 0{\cdot}1$ s, $\alpha = 10^{-6}$.

For linearly ($s = 1$) and parabolically ($s = 2$) tapered plates the optimal values equal $h_{2opt} = 0{\cdot}34$ and $h_{2opt} = 0{\cdot}52$, respectively. In both cases, the minimal critical forces ($P_{cr} = 131{\cdot}9$ and $P_{cr} = 143{\cdot}5$) are connected with the first eigenvalues of vibration and $m = 0$ (see Figure 11). The critical forces obtained for $m = 1$–4 are greater than the previous ones.

As also shown in Figure 11, for $s = 3$ one has quite different phenomena. The lowest critical force obtained for $m = 0$ increases with increasing values of parameter h_2 and reaches the value $P_{cr} = 180{\cdot}6$ for $h_2 = 0{\cdot}84$. For greater values of h_2, the critical force jumps

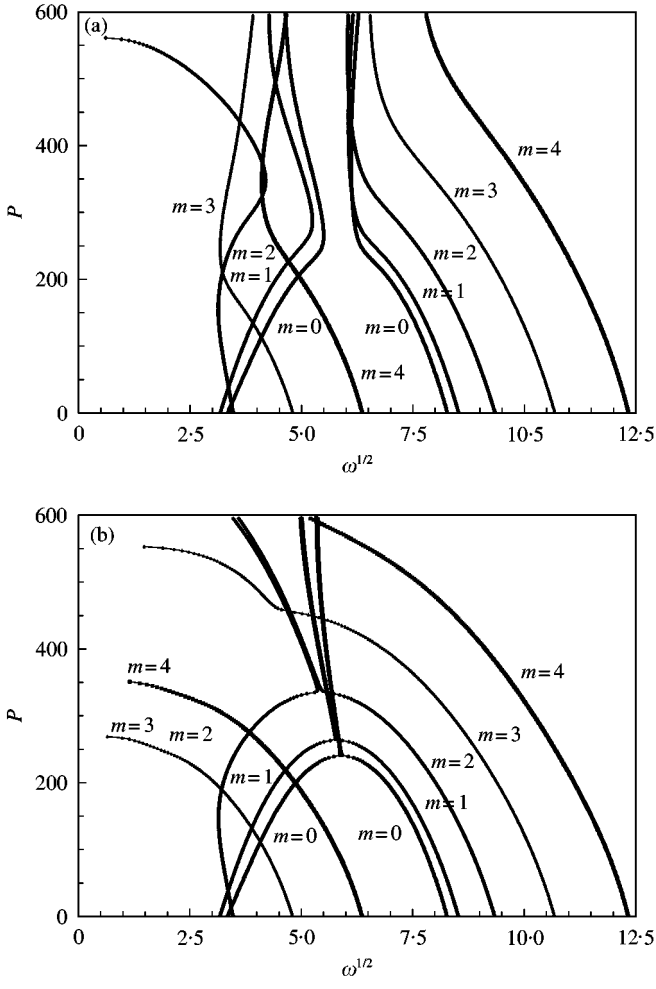

Figure 9. Compressive force versus the imaginary part of the first and second frequencies with various values of m, for (a) $\bar{\tau} = 0{\cdot}1$ s and (b) $\bar{\tau} = 10$ s.

to level $P_{cr} = 369{\cdot}6$ for $h_2 = 0{\cdot}85$. Simultaneously, the critical force obtained for $m = 4$ rapidly decreases from $P_{cr} = 201{\cdot}6$ for $h_2 = 0{\cdot}83$ to $P_{cr} = 177{\cdot}6$ for $h_2 = 0{\cdot}84$ and $P_{cr} = 155{\cdot}4$ for $h_2 = 0{\cdot}85$.

Therefore, for $s = 3$ and $h_2 = 0{\cdot}839$, the bimodal optimal solution has been obtained for which the critical forces P_0 and P_4 are the same for $m = 0$ and 4 as seen in Figure 12. Similar phenomena have been observed for $s = 4{\cdot}5$, where for $h_2 = 0{\cdot}847$ one has $P_0 = P_6 = 218$ for $m = 0$ and 6 as seen in Figure 13.

7. CONCLUSIONS

1. The characteristic curves for the annular plate compressed by a tangential force in non-linear creep conditions have been analyzed for the first time.

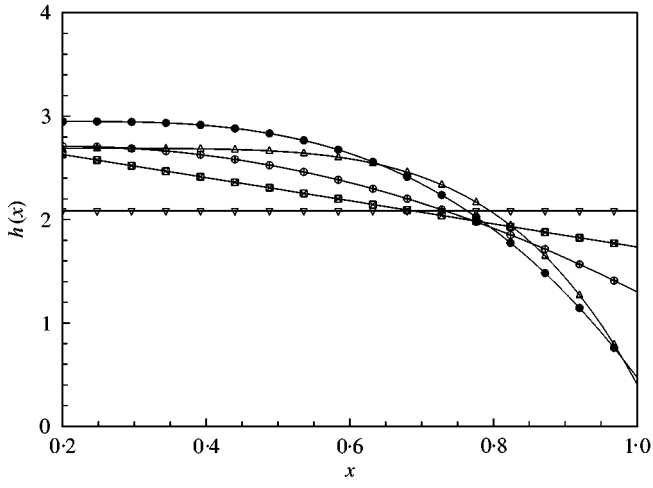

Figure 10. Thickness of the non-uniform plates, key for s and h_2 values respectively: ■—■, 1/0·34; ⊕—⊕, 2/0·52; ●—●, 3/0·839; △—△, 4·5/0·847 and ▽—▽, $h_2 = 0$.

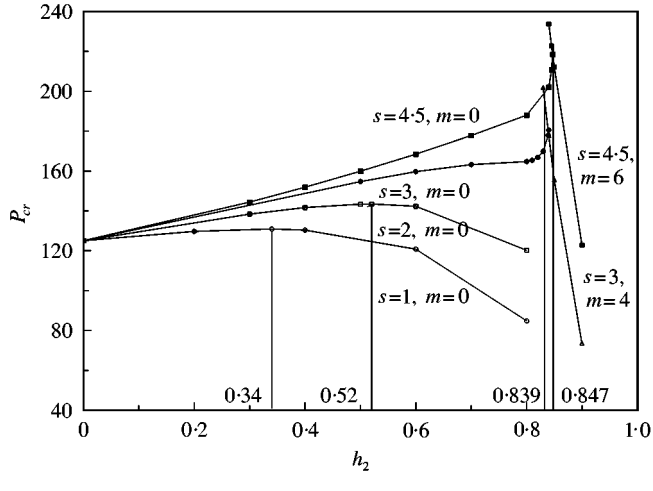

Figure 11. Critical compressive force versus parameter h_2, for $\alpha = 10^{-6}$ and $\bar{\tau} = 0{\cdot}1$ s. Curve numbers refer to s and m values respectively.

2. The destabilization phenomenon due to a non-linear creep of material has been observed. Although, as yet, the destabilizing effect of damping has not been verified experimentally (see e.g., reference [12]) this effect should be taken into account in further considerations. As seen in Figure 8 the real parts δ_1 reach high positive values, which can lead to the loss of stability in a short time (not only after infinite time).
3. In a parametrical optimization procedure, the bimodal optimal solutions have been obtained. For the "bimodal optimal shape", the critical forces are the same for various values of circumferential waves.
4. The results presented in the paper are different from those obtained for columns.

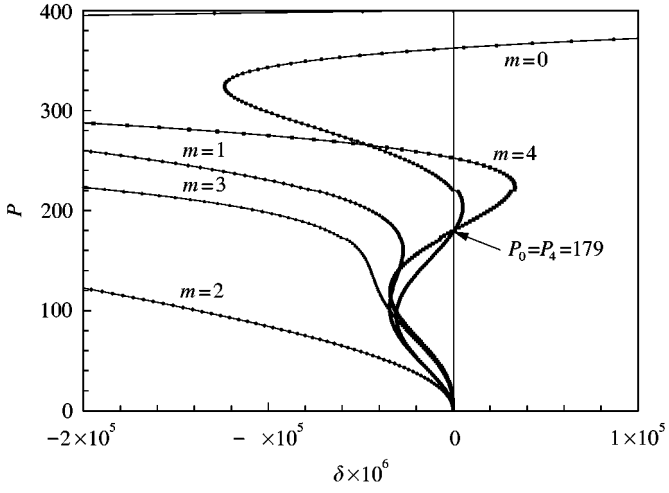

Figure 12. Bimodal critical force for s = 3, $h_2 = 0{\cdot}839$, $\alpha = 10^{-6}$ and $\bar{\tau} = 0{\cdot}1$ s. Curve labels indicate m values.

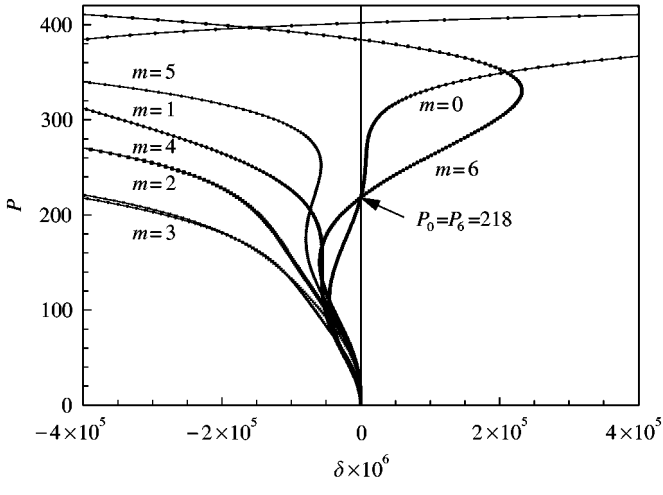

Figure 13. Bimodal critical force for s = 4·5, $h_2 = 0{\cdot}847$, $\alpha = 10^{-6}$ and $\bar{\tau} = 0{\cdot}1$ s. Curve labels indicate m values.

ACKNOWLEDGMENT

Partial support of this work under Grant 7-T07A-031-16 by the Committee for Scientific Research is gratefully acknowledged.

REFERENCES

1. M. BECK 1952 *Zeitschrift für Angewandte Mathematik und Mechanik* **3**, 225–228. Die Knicklast des einseitig eingespannten tangential gedrückten Stabes.
2. A. GAJEWSKI and M. ŻYCZKOWSKI 1988 *Optimal Structural Design under Stability Constraints.* Dordrecht: Kluwer Academic Publishers.

3. R. BOGACZ and R. JANISZEWSKI 1987 *Advances in Mechanics* (*Uspekhi Mekhaniki*) **8**, 3–52 Analysis and synthesis of column under follower forces from the point of view of stability. (in Russian).
4. M. A. LANGTHJEM and Y. SUGIYAMA 1999 *Journal of Sound and Vibration* **226** (1), 1–23. Optimum shape design against flutter of a cantilevered column with an end-mass of finite size subjected to a non-conservative load.
5. M. A. LANGTHJEM and Y. SUGIYAMA 2000 Computers and Structures **74**, 385–398. Optimum design of cantilevered columns under the combined action of conservative and nonconservative loads. Part I: the undamped case.
6. M. A. LANGTHJEM and Y. SUGIYAMA 2000 Computers and Structures **74**, 399–408. Optimum design of cantilevered columns under the combined action of conservative and nonconservative loads. Part II: the damped case.
7. W. T. KOITER 1996 *Journal of Sound and Vibration* **194**, 636. Unrealistic follower forces.
8. YU. I. YAGN and L. K. PARSHIN 1967 *Prochnost materyalov i konstruktziy* (*Strength of materials and structures*), *Trudy LPI* (*Works of Leningrad Technical Institute*), No. 278, 52–54. Experimental verification of stability of a column compressed by a follower force (in Russian).
9. Y. SUGIYAMA, K. KATAYAMA and S. KINOI 1995 *Journal of Aerospace Engineering*, *American Society of Civil Engineers* **8**, 9–15. Flutter of cantilevered column under rocket thrust.
10. Y. SUGIYAMA, K. KATAYAMA, K. KIRIYAMA and B.-J. RYU 2000 *Journal of Sound and Vibration* **236**, 193–207. Experimental verification of dynamic stability of vertical cantilevered columns subjected to a sub-tangential force.
11. M. A. LANGTHJEM, Y. SUGIYAMA, M. KOBAYASHI and H. YUTANI 2000 Fourth *EUROMECH Solid Mechanics Conference*, *Metz*, *France*, *June 26–30*, *Book of Abstracts II* 662. Experimental verification of optimization of cantilevered columns subjected to a rocket thrust.
12. Y. SUGIYAMA, M. A. LANGTHJEM and B.-J. RYU 1999 *Journal of Sound and Vibration* **225**, 779–782. Realistic follower forces. Letters to the Editor.
13. T. IRIE, G. YAMMADA and Y. KANEKO 1980 *Journal of Sound and Vibration* **73**, 261–269. Vibration and stability of a non-uniform annular plate subjected to a follower force.
14. A. GAJEWSKI and P. CUPIAŁ 1992 *International Journal of Solids Structures* **29**, 1283–1292. Optimal structural design of an annular plate compressed by non-conservative forces.
15. A. GAJEWSKI 1997 In: *Proceedings of the Second World Congress of Structural and Multidisciplinary Optimization*, (W. GUTKOWSKI and Z. MRÓZ, editors), Zakopane, Poland, May 26–30, 737–742. Optimization of a column compressed by non-conservative force in non-linear creep contions.
16. A. GAJEWSKI 2000 *Journal of Theoretical and Applied Mechanics* **38**, 259–270. Vibrations and stability of a non-conservatively compressed prismatic column under non-linear creep conditions.
17. M. ŻYCZKOWSKI 1996 *Applied Mechanics Reviews* **49**, 433–446. Optimal structural design under creep conditions.
18. A. WRÓBLEWSKI 1992 *Engineering Optimization* **20**, 111–128. Optimal design of circular plates against creep buckling.
19. C. C. DAVENPORT 1938 *Journal of Applied Mechanics* **5**, A55–A60. Correlation of creep and relaxation properties of copper.
20. YU. N. RABOTNOV and S. A. SHESTERIKOV 1957 *Prikladnaya Matematika i Mekhanika* **21**, 406–412 (Russian version), *Journal of Mechanics and Physics of Solids* **6**, 27–34 (English version). Creep stability of columns and plates.
21. A. WRÓBLEWSKI and M. ŻYCZKOWSKI 1989 *Structural Optimization* **1**, 227–234. On multimodal optimization of circular arches against plane and spatial creep buckling.
22. YU. N. RABOTNOV 1966 *Creep of Structural Elements.* Moskva, Nauka (in Russian).
23. A. M. ZHUKOV, Yu. N. RABOTNOV and F. S. CHURIKOV 1953 *Inzhenernyi Sbornik* **17**, 163–170. Experimental verification of some theories of creep (in Russian).
24. V. B. GRINEV and A. P. FILIPPOV 1977 *Stroitelna Mekhanika i Raschot Sooruzheniy* **2**, 16–20. Optimal design of circular plates in stability problems (in Russian).